

AFOSR TR 97-0695

REPORT DOCUMENTATION PAGE			Form Approved OMB No. 0704-0188	
<small>Public reporting burden for this collection of information is estimated to average 1 hour per response, including the time for reviewing instructions, searching existing data sources, gathering and maintaining the data needed, and completing and reviewing the collection of information. Send comments regarding this burden estimate or any other aspect of this collection of information, including suggestions for reducing this burden, to Washington Headquarters Services, Directorate for Information Operations and Reports, 1215 Jefferson Davis Highway, Suite 1204, Arlington, VA 22202-4302, and to the Office of Management and Budget, Paperwork Reduction Project (0704-0100), Washington, DC 20503.</small>				
1. AGENCY USE ONLY (Leave blank)	2. REPORT DATE	3. REPORT TYPE AND DATES COVERED		
		Final 31 Aug 94 to 30 Aug 97		
4. TITLE AND SUBTITLE		5. FUNDING NUMBERS		
(ASSERT 94-108) MEASUREMENT OF THE LINEWIDTH ENHANCEMENT FACTOR AT HIGH EXCITATION LEVELS		61103D 3483/TS		
6. AUTHOR(S)				
Professor Brueck				
7. PERFORMING ORGANIZATION NAME(S) AND ADDRESS(ES)		8. PERFORMING ORGANIZATION REPORT NUMBER		
University of New Mexico Office of Research Admin 102 Scholes Hall Albuquerque NM 87131-6003				
9. SPONSORING/MONITORING AGENCY NAME(S) AND ADDRESS(ES)		10. SPONSORING/MONITORING AGENCY REPORT NUMBER		
AFOSR/NE 110 Duncan Ave RoomB115 Bolling AFB DC 20332-8050		F49620-94-1-0301		
11. SUPPLEMENTARY NOTES				
12a. DISTRIBUTION/AVAILABILITY STATEMENT			12b. DISTRIBUTION CODE	
APPROVAL FOR PUBLIC RELEASED: DISTRIBUTION UNLIMITED				
13. ABSTRACT (Maximum 200 words)				
<p>We have undertaken the first systematic investigation of the impact of the quantum well epitaxial structure on the <math>\alpha</math>-parameter in broad-area quantum well lasers. Modal gain, carrier-induced refractive index change, and a parameter have been measured in quantum wells of varying width, depth, and material composition using four structures: 60 Å and 500 Å GaAs quantum wells, referred to as "narrow" and "wide", and 60 Å InGaAs wells with AlGaAs barriers of two different aluminum concentrations giving "shallow" and "deep" wells.</p>				
14. SUBJECT TERMS			15. NUMBER OF PAGES	
			16. PRICE CODE	
17. SECURITY CLASSIFICATION OF REPORT	18. SECURITY CLASSIFICATION OF THIS PAGE	19. SECURITY CLASSIFICATION OF ABSTRACT	20. LIMITATION OF ABSTRACT	
UNCLASSIFIED	UNCLASSIFIED	UNCLASSIFIED	UL	

NSN 7540-01-280-5500

Standard Form 298 (Rev. 2-89)  
Prescribed by ANSI Std. Z39-18

DTIC QUALITY INSPECTED 4

**ATTACHMENT**  
**AUGMENTATION AWARDS FOR SCIENCE & ENGINEERING RESEARCH TRAINING**  
**(AASERT)**  
**REPORTING FORM**

The Department of Defense (DoD) requires certain information to evaluate the effectiveness of the AASERT Program. By accepting this Grant which bestows the AASERT funds, the Grantee agrees to provide 1) a brief (not to exceed one page) narrative technical report of the research training activities of the AASERT-funded student(s) and 2) the information requested below. This information should be provided to the Government's technical point of contact by each annual anniversary of the AASERT award date.

**1. Grantee Identification data: (R&T and Grant numbers found on Page 1 of Grant)**

- a. The Regents of the University of New Mexico  
**University Name**
- b. F49620-94-1-0301  
**Grant Number**
- c. \_\_\_\_\_  
**R&T Number**
- d. S.R.J. Brueck  
**P.I. Name**
- e. From: 31 Aug 96 - To: 30 Aug 97  
**AASERT Reporting Period**

**NOTE: Grant to which AASERT award is attached is referred to hereafter as "Parent Agreement".**

**2. Total funding of the Parent Agreement and the number of full-time equivalent graduate students (FTEGS) supported by the Parent Agreement during the 12-month period prior to the AASERT award date.**

- a. **Funding:** \$ 600,000
- b. **Number FTEGS:** 6

**3. Total funding of the Parent Agreement and the number of FTEGS supported by the Parent Agreement during the current 12-month reporting period.**

- a. **Funding:** \$ 1,829,028
- b. **Number FTEGS** 11

**4. Total AASERT funding and the number of FTEGS and undergraduate students (UGS) supported by AASERT funds during the current 12-month reporting period.**

- a. **Funding:** \$ 118,306
- b. **Number FTEGS:** 1
- c. **Number UGS:** -

**VERIFICATION STATEMENT:** I hereby verify that all students supported by the AASERT award are U.S. Citizens.

  
\_\_\_\_\_  
**Principal Investigator**

11/21/97  
\_\_\_\_\_  
**Date**

**Final Report**

**Measurement of the Linewidth Enhancement Factor  
at High Excitation Levels**

**Contract # F49620-94-1-0301**

**For the Period  
31 Aug 94 - 30 Aug 97**

**Submitted by:**

**Professor S. R. J. Brueck  
Center for High Technology Materials  
University of New Mexico  
Albuquerque, NM 87106**

**voice: (505) 272-7800; fax: (505) 272-7801; email: brueck@chtm.unm.edu**

19971204 110

## **Dependence of Linewidth Enhancement Factor on Quantum Well Width and Depth in GaAs and InGaAs Broad-Area Lasers**

Jonathan Stohs, David J. Bossert, David J. Gallant, S. R. J. Brueck

Jonathan Stohs, Center for High Technology Materials, University of New Mexico, EECE Bldg., Rm. 125, Albuquerque, NM 87131. Phone: (505) 846-1921 Fax: (505) 846-4313  
e-mail: stohs@chtm.unm.edu

David J. Bossert, Semiconductor Laser Branch, Phillips Lab., 3550 Aberdeen Ave. SE, Kirtland AFB, NM 87117

David J. Gallant, Rockwell Power Systems, P.O. Box 5670, Kirtland AFB, NM 87185

S. R. J. Brueck, Center for High Technology Materials, University of New Mexico, 1313 Goddard SE, Albuquerque, NM 87106.

### **Summary:**

This is a joint program involving collaboration between the Air Force's Phillips Laboratory and the University of New Mexico. To date, the majority of the experimental work has been carried out at the Phillips Laboratory by a UNM graduate student (Stohs). Analysis of the data is being carried out jointly.

The spatial coherence and filamentation tendencies of high-power semiconductor lasers are strongly influenced by the linewidth enhancement factor,  $\alpha$  which is also a critical parameter controlling the linewidth and modulation characteristics of high frequency diode lasers.

We have undertaken the first systematic investigation of the impact of the quantum well epitaxial structure on the  $\alpha$ -parameter in broad-area quantum well lasers. Modal gain, carrier-induced refractive index change, and a parameter have been measured in quantum wells of varying width, depth, and material composition using four structures: 60 Å and 500 Å GaAs quantum wells, referred to as "narrow" and "wide", and 60 Å InGaAs wells with AlGaAs barriers of two different aluminum concentrations giving "shallow" and "deep" wells.

### Experiment:

The modal gain and refractive index change with injection current were determined from the depth of modulation and wavelength shift of below-threshold amplified spontaneous emission spectra [1] obtained with a monochromator and photomultiplier tube. A far-field spatial filter was used to eliminate all but the fundamental lateral mode. Additionally, the output facets of our tested devices were anti-reflection coated, increasing the below-threshold current range.

By measuring the wavelength shift with current density,  $d\lambda/dJ$ , and the gain change,  $dg/dJ$ , between amplified spontaneous emission spectra at two current densities  $J$  and  $J + dJ$  the linewidth enhancement factor is calculated according to [2,3]

$$\alpha = -2k \frac{\delta n}{\delta g} = \left( \frac{-2\pi}{L\Delta\lambda} \right) \frac{\delta\lambda/\delta J}{\delta g/\delta J} \quad (1)$$

where  $k$  is the wavenumber, and  $\delta n$  and  $\delta g$  are the refractive index and gain changes between injection current densities  $J$  and  $J + \delta J$ , and  $\Delta\lambda$  is the free spectral range of the laser cavity. The index change with current density is proportional to the measured wavelength shift.

### Results:

Figures 1 and 2 show the measurement results for the four device structures studied. It is evident from Fig. 2 that the lowest values of  $\alpha$  occur in the narrow GaAs and deep InGaAs wells. In the GaAs narrow well  $\alpha$  is about 3 and decreases to about 2 at higher current densities. The GaAs wide well has a values that start at about 6 and decrease to about 2.5. The InGaAs deep well displays  $\alpha$  values of approximately 2, which is similar to the GaAs narrow well. In the InGaAs shallow well we see from Fig. 1 that surprisingly large values of  $\alpha$  occur for current densities above 300 A/cm<sup>2</sup>.

The strong influence of well depth on  $\alpha$ , evident in Fig. 1, (for the case of deep and shallow InGaAs wells) can be traced to large refractive index changes with current. For the InGaAs shallow well the index change is significantly larger than that of the deep well due to the large population in the barrier energy levels above the quantum well. Carriers with energies above the quantum well barrier height can be referred to as "off-resonant" in that they do not contribute to gain, which is dominated by optical transitions from energy levels in the quantum well itself, but do in fact contribute to changes in the modal refractive index. The high  $\alpha$  values for the shallow well, as seen in Fig. 1, are caused by these "off-resonant" carriers as demonstrated by our observation that the differential gain is about the same as for the deep well,

but the differential index change is much larger (see Eq. 1). Since the deep well has barrier energy levels which are much less populated with carriers, its differential index change is much smaller, resulting in lower  $\alpha$ . Further detailed discussion of these results can be found in the presentation given at the February SPIE conference and attached as Appendix A: "Epitaxial structure dependence of the linewidth enhancement factor in GaAs and InGaAs quantum well lasers", Proc. SPIE; *Physics and Simulation of Optoelectronic Devices V*; vol. **2994**, pp. 542-551, Feb. 1997 (San Jose).

#### **Future Work:**

Over the next year, we plan a comparison of these below-threshold measurements of  $\alpha$  to those made using another experimental technique, such as modulating the carrier density in a traveling wave amplifier and determining the resultant signal AM and FM [4], to more completely characterize the structural dependence of  $\alpha$  over wide current and frequency ranges.

#### **References:**

- [1] D. J. Bossert, D. Gallant, *Electron. Lett.* **32**, 4 (1996).
- [2] B. W. Hakki, T. L. Paoli, *J. Appl. Phys.* **46**, 3 (1974).
- [3] I. D. Henning, J. V. Collins, *Electron. Lett.* **19**, 22 (1983).
- [4] N. Storkfelt, B. Mikkelsen, et. al., *IEEE Phot. Tech. Lett.* **3**, 7 (1991).

## Appendix A

### **Epitaxial Structure Dependence of the Linewidth Enhancement Factor in GaAs and InGaAs Quantum Well Lasers**

Jonathan Stohs, David J. Gallant, David J. Bossert, and Steven R. J. Brueck  
Proceedings SPIE 2994, *Physics and Simulation of Optoelectronic Devices V*, 542-551 (1997).

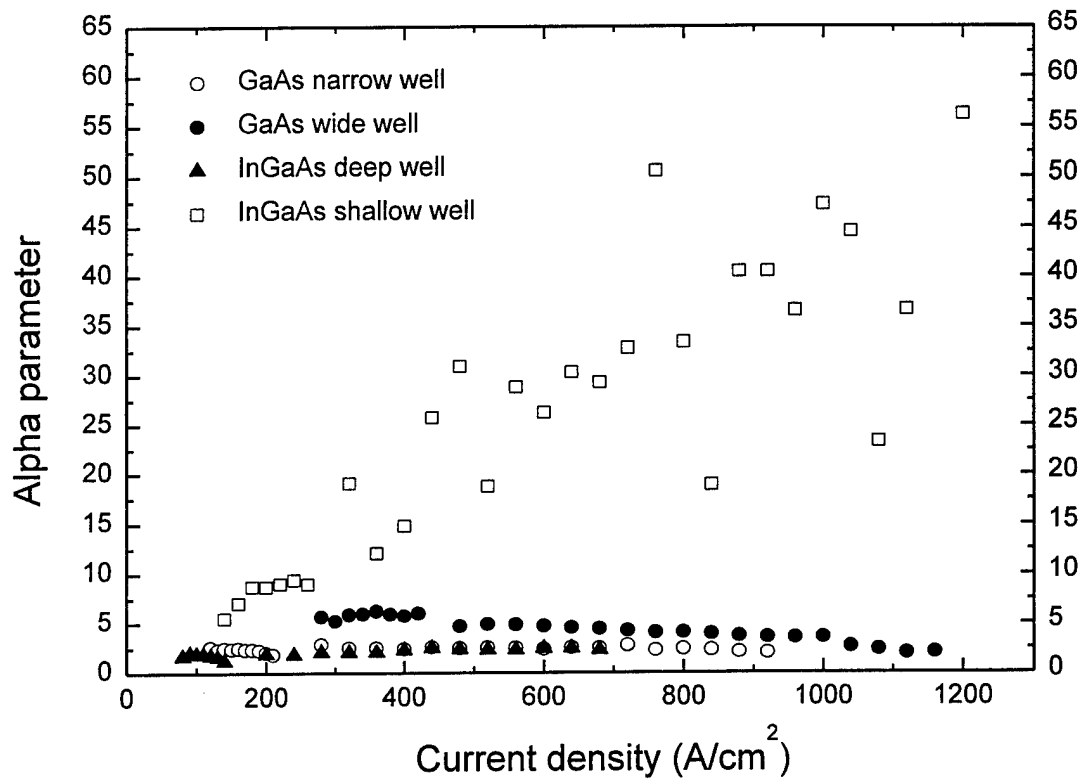


Figure 1. Alpha vs current density for all four quantum wells.

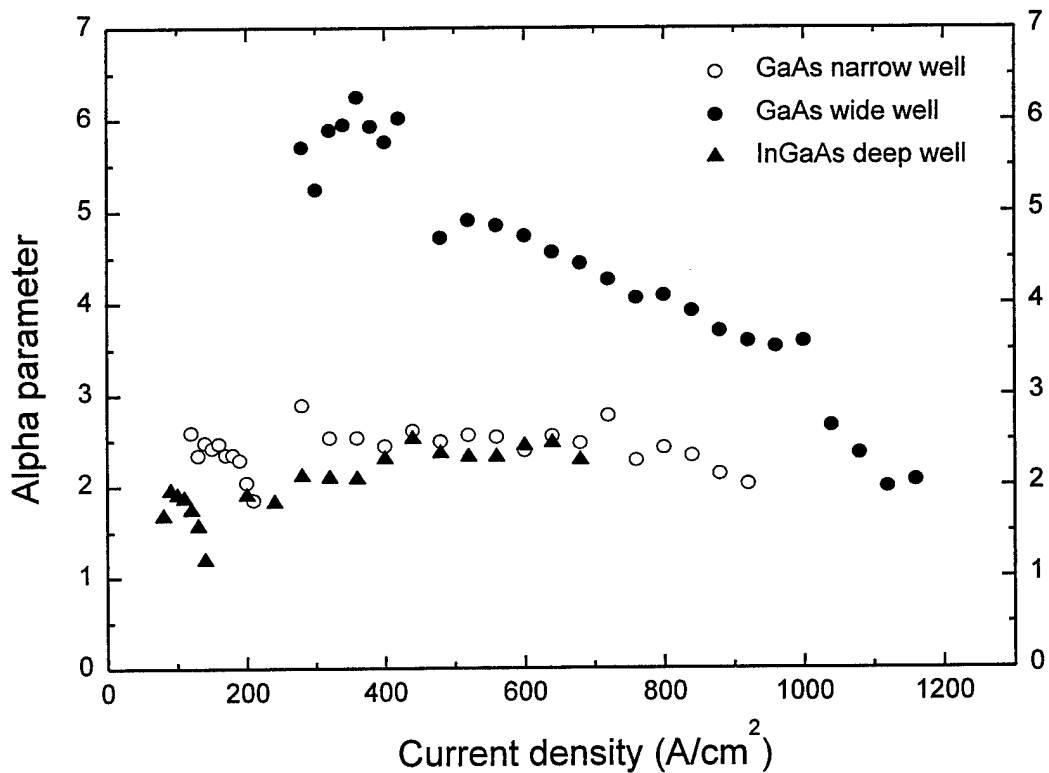


Figure 2. Same graph as above, but without the shallow well.

## Appendix A

### **Epitaxial Structure Dependence of the Linewidth Enhancement Factor in GaAs and InGaAs Quantum Well Lasers**

Jonathan Stohs, David J. Gallant, David J. Bossert, and Steven R. J. Brueck  
Proceedings SPIE **2994**, *Physics and Simulation of Optoelectronic Devices V*, 542-551 (1997).

# Epitaxial Structure Dependence of the Linewidth Enhancement Factor in GaAs and InGaAs Quantum Well Lasers

Jonathan Stohs<sup>1</sup>, David J. Gallant<sup>2</sup>, David J. Bossert<sup>3</sup>, and Steven R. J. Brueck<sup>1</sup>

- (1) Center for High Technology Materials, University of New Mexico, EECE Bldg., Rm. 125, Albuquerque, NM 87131
- (2) Rocketdyne Technical Services, P. O. Box 5670, Kirtland AFB, NM 87185
- (3) Semiconductor Laser Branch, Phillips Lab., 3550 Aberdeen Ave. SE, Kirtland AFB, NM 87117

## ABSTRACT

The linewidth enhancement factor,  $\alpha$ , plays a key role in our ability to obtain spatially coherent output from high-power semiconductor lasers and amplifiers. To obtain  $\alpha$  values, modal gain and carrier-induced refractive index change have been measured in broad-area quantum well epitaxial structures with various well depths, widths, and compositions as functions of current density.

**Keywords:** linewidth enhancement factor, differential gain, index shift, quantum well lasers

## 1. INTRODUCTION

The linewidth enhancement factor,  $\alpha$ , which describes the coupling of carrier-induced gain and index changes, is an important parameter in the design of semiconductor lasers. The spatial coherence and filamentation tendencies of broad-area, high-power semiconductor lasers and amplifiers are strongly influenced by the linewidth enhancement factor. In addition, the linewidth and modulation characteristics of diode lasers are also directly dependent on  $\alpha$ . We report here the results of an experimental investigation carried out to determine the epitaxial structural dependencies, specifically well depth and width, of  $\alpha$  in GaAs and InGaAs quantum well lasers. Modal gain, differential gain, and wavelength shift, which is proportional to refractive index change, were measured versus current density. We find a substantial dependence of the  $\alpha$  parameter on the epitaxial structure. In general, deeper, narrower quantum wells give markedly lower values of  $\alpha$ .

## 2. MEASURING THE $\alpha$ PARAMETER

The  $\alpha$  parameter is defined as<sup>1</sup>

$$\alpha = -2 \frac{2\pi}{\lambda} \frac{\delta n / \delta N}{\delta g / \delta N} \quad (1)$$

where  $2\pi/\lambda$  is the free space wave vector,  $\delta n/\delta N$  is the change in refractive index with carrier density, and  $\delta g/\delta N$  is the change in gain with carrier density. With a small change in injected current density in a

semiconductor laser, the Fabry-Perot mode peaks are observed to shift an amount  $\delta\lambda$ . The corresponding change in the index of refraction is given by

$$\delta n = \frac{n_g}{\lambda} \delta\lambda \quad (2)$$

where  $n_g$  is the group index. The mode spacing  $\Delta\lambda$  in a Fabry-Perot cavity is given by

$$\Delta\lambda = \frac{\lambda^2}{2n_g L} \quad (3)$$

where  $L$  is the cavity length. Using (2) and (3) in (1) we can express  $\alpha$  as

$$\alpha = \left( \frac{-2\pi}{L\Delta\lambda} \right) \frac{\delta\lambda/\delta N}{\delta g/\delta N} \quad (4)$$

If we assume, for small changes, that the carrier density change  $\delta N$  is proportional to the current density change  $\delta J$  then

$$\alpha = \left( \frac{-2\pi}{L\Delta\lambda} \right) \frac{\delta\lambda/\delta J}{\delta g/\delta J} \quad (5)$$

and we have an equation for  $\alpha$  in terms of experimentally measurable quantities. The net modal power gain  $g$  is found according to<sup>2,3</sup>

$$g = \frac{1}{L} \ln \left( \frac{\sqrt{\rho} - 1}{\sqrt{\rho} + 1} \right) + \frac{1}{2L} \ln \frac{1}{R_1 R_2} \quad (6)$$

where  $L$  is the laser cavity length,  $\rho$  is the ratio of the intensity maximum to the intensity minimum in the below-threshold amplified spontaneous emission (ASE) spectrum, and  $R_1$  and  $R_2$  are the semiconductor laser facet reflectivities.

Below-threshold ASE spectral measurements were used to determine changes in gain and wavelength shifts due to small changes in injected current. A temperature-controlled mount kept at 20 °C and low duty cycle current pulses minimized any heating effects within the lasers. The laser output was directed into a monochromator with a cooled photomultiplier tube. Broad-area lasers were used in this study, and a far-field filtering technique was employed to select a single plane wave mode propagating perpendicular to the facets. This eliminated  $\alpha$  parameter dependencies on the lateral waveguiding and carrier confinement structure.<sup>4</sup> Other experimental details are further described in Ref. 4. Low current data were taken on devices with uncoated facets. Higher current data were taken after anti-reflection coating the output facet of each device, to a reflectivity of about  $10^{-3}$ , to allow measurements at higher currents before the onset of lasing. This allowed data to be obtained at carrier densities where high-brightness semiconductor lasers and amplifiers typically operate.

### 3. QUANTUM WELL STRUCTURES

In this study we examined the influence of quantum well width and depth on measured  $\alpha$  values. The quantum well lasers were grown using MOCVD and processed into devices with 50  $\mu\text{m}$  stripe widths and cavity lengths of 500  $\mu\text{m}$ . The first two quantum well structures studied are shown in Fig. 1. These have GaAs active regions between barriers of  $\text{Al}_{0.3}\text{Ga}_{0.7}\text{As}$ . The 60 Å and 500 Å wide quantum wells will be referred to as "narrow" and "wide" respectively. The peak of the ASE spectrum for the narrow well had a wavelength of 803 nm and for the wide well it was 880 nm.

The second pair of laser structures is shown in Fig. 2 where the quantum well depth is varied between the two. These devices have  $\text{In}_{0.2}\text{Ga}_{0.8}\text{As}$  active regions, and the aluminum concentration in the barriers is varied to effect "shallow" and "deep" wells. The barrier composition for the deep well is  $\text{Al}_{0.2}\text{Ga}_{0.8}\text{As}$  and for the shallow well it is GaAs. In the case of the deep well the wavelength of the ASE spectrum peak is 906 nm and that of the shallow well is 950 nm.

Electroluminescence spectra and a computer model were utilized to determine quantum well energy levels, taking into account strain for the InGaAs wells, and using layer thickness and indium concentration as parameters.<sup>5,6</sup> Based on our analyses, the deep and shallow wells were found to have active regions with nominal thickness and indium concentration of  $55 \text{ \AA} \pm 2 \text{ \AA}$  and  $15\% \pm 2\%$  respectively.

#### 4. NARROW AND WIDE GaAs WELLS

The measured gain as a function of current density for the narrow and wide well devices is shown in Fig. 3. Data were taken at the peak wavelength of the ASE spectrum. Since the ASE peak shifts with current due to band filling effects, the ASE peak was automatically tracked by the data acquisition system as the current was increased. From the data it can be seen that the wide well achieves transparency and threshold at higher current densities than the narrow well. In addition, the narrow well shows definite gain saturation above  $400 \text{ A/cm}^2$  due to carriers filling up the states available at the energy level involved in the optical transition. The wide well shows a more linear increase in gain, typical of double heterostructure lasers, up to  $1000 \text{ A/cm}^2$ . Note that with a width of  $500 \text{ \AA}$  the wide well is nearly a double heterostructure device.

The differential gain is plotted in Fig. 4 as a function of injected current density. As can be seen, the differential gain for the narrow well decreases more quickly than the wide well as a result of the prominent gain saturation of the narrow well at higher injection levels.

In Fig. 5 the magnitude of the differential wavelength shift, or equivalently, the refractive index change with carrier density (see Eq. 2), is plotted. The wavelength shift was found to be larger for the wide well than for the narrow well. The increased number of states in the wide well and its greater spatial overlap with the mode allow a larger number of "nonresonant" carriers to contribute to the modal index than in the narrow well case.

The  $\alpha$  parameter for the narrow and wide wells, derived from the differential gain and wavelength shift data, is plotted in Fig. 6. For the narrow well  $\alpha$  remains mostly constant at a value of 2.5, decreasing slightly with current density. We see that  $\alpha$  for the wide well is significantly higher than for the narrow well at lower injection levels and decreases strongly with injection level. The increased  $\alpha$  values for the wide well are predominantly a result of the increased differential wavelength (index) shift. As the injection level is increased, the wide well wavelength shift decreases faster than the differential gain, resulting in a decreasing value of  $\alpha$ .

#### 5. DEEP AND SHALLOW InGaAs WELLS

Measured gain data for the deep and shallow InGaAs quantum wells is presented in Fig. 7. It is evident from Fig. 7 that the gain for each well increases rapidly at lower current densities, but at  $300 \text{ A/cm}^2$  the gain of the shallow well begins to saturate more quickly than the deep well. In Fig. 8 the differential gains for these wells are shown. The differential gains of the deep and shallow wells do not differ significantly, however, the differential gain for the deep well is higher, as expected from the gain measurements. Both differential gain curves decrease with injection current, reflecting the saturation of the gain.

In Fig. 9 the differential wavelength shifts (refractive index changes) for the deep and shallow wells are shown. It can be seen that the wavelength shifts of the shallow well are much greater than those of the deep well by a factor of 2-3. Evidently, the refractive index change is more pronounced in the shallow well due to differences in quantum well energy levels. In the shallow well there exists a single energy level below the barrier energy states whereas in the deep well there are two. When carriers have filled the states in the single energy level in the shallow well, additional carriers populate the barrier states. These nonresonant carriers are no longer confined to the well region and therefore have wavefunctions with

larger spatial extent, allowing a greater interaction with the optical mode and leading to increased index change or wavelength shift. In the deep well, once the states in the lowest energy level in the well are filled, additional carriers populate the second energy level before they are likely to exist in barrier states.

The  $\alpha$  values for the deep and shallow wells are plotted versus current density in Fig. 10. For the deep well, measured values of  $\alpha$  remain near 2 throughout the current density range studied. Even though the differential gain for the deep well decreases, the differential wavelength shift diminishes proportionately, keeping a nearly constant value of  $\alpha$ .

While the  $\alpha$  values are quite low for the deep well, the  $\alpha$  values for the shallow well increase quickly with current density becoming a factor of 15 to 20 greater than for the deep well. Since the wavelength shifts for the shallow well in Fig. 9 are much higher than for the deep well, and the differential gain values in Fig. 8 are similar to those of the deep well, it is evident that the large increase in  $\alpha$  values for the shallow well is due predominantly to its greater wavelength shifts. As current is increased in the shallow well device, carriers fill up available states ( $n=1$ ) in the well, decreasing the differential gain. At higher current densities additional carriers begin to populate energy states in the barrier region above the well.<sup>7</sup> These "nonresonant" carriers do not contribute to gain at the measured wavelength, but still contribute to refractive index change, increasing the  $\alpha$  parameter.

## 6. CONCLUSION

We have measured the modal gain and carrier-induced refractive index changes in broad-area quantum well structures. Quantum well epitaxial structures were varied to examine the influence of quantum well structure on the  $\alpha$  parameter. We have seen from the data presented here that the  $\alpha$  parameter in quantum well lasers is significantly influenced by quantum well width and depth. Data for narrow and wide GaAs wells demonstrate that wide wells have a larger  $\alpha$  parameter than narrow ones due to larger wavelength shifts resulting from an increase in the number of states available in the well and the increased spatial overlap with the mode.

It is also apparent that the depth of a quantum well plays a major role in determining its gain behavior and especially its index change characteristics. In the shallow well, carrier population of energy states above the well in the barrier leads to large refractive index changes and correspondingly large wavelength shifts. This population of barrier states by nonresonant carriers along with low differential gain at higher current densities are factors which result in large  $\alpha$  values. In the deep well case, which had much smaller wavelength shifts and somewhat larger differential gains, the  $\alpha$  parameter is lower and remains essentially constant over the range of current densities studied.

## REFERENCES

- [1] M. Osinski and J. Buss, "Linewidth broadening factor in semiconductor lasers - an overview", *IEEE J. Quantum Electron.*, QE-23, 1, pp. 9-29, Jan. 1987.
- [2] B. W. Hakki and T. L. Paoli, "CW degradation at 300 K of GaAs double-heterostructure junction lasers, II, electronic gain", *J. Appl. Phys.*, 44, 9, pp. 4113-4119, Sept. 1973.
- [3] B. W. Hakki and T. L. Paoli, "Gain spectra in GaAs double-heterostructure injection lasers", *J. Appl. Phys.*, 46, 3, pp. 1299-1306, Mar. 1975.
- [4] D. J. Bossert and D. Gallant, "Improved method for gain/index measurements of semiconductor lasers", *Electron. Lett.*, 32, 4, pp. 338-339, 15 Feb. 1996.

- [5] B. Jonsson and S. T. Eng, "Solving the Schroedinger equation in arbitrary quantum well potential profiles using the transfer matrix method", *IEEE J. Quantum Electron.*, QE-26, 11, pp. 2025-2035, Nov. 1990.
- [6] G. Ji, D. Huang, U. K. Reddy, T. S. Henderson, R. Houdré, and H. Morkoc, "Optical investigation of highly strained InGaAs-GaAs multiple quantum wells", *J. Appl. Phys.*, 62, 8, pp. 3366-3373, 15 Oct. 1987.
- [7] A. P. Ongstad, D. J. Gallant, and G. C. Dente, "Carrier lifetime saturation in InGaAs single quantum wells", *Appl. Phys. Lett.*, 66, 20, pp. 2730-2732, 15 May 1995.

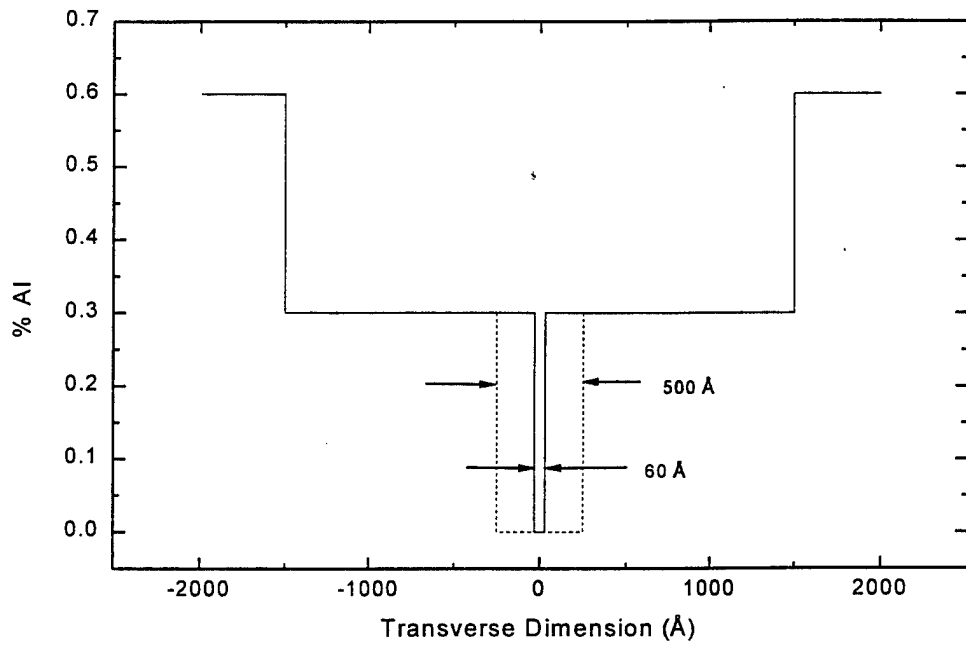


**Figure 1.** Material compositions and layer thicknesses of narrow and wide GaAs quantum wells. The narrow well is indicated by the solid line, and the wide well by the dashed line

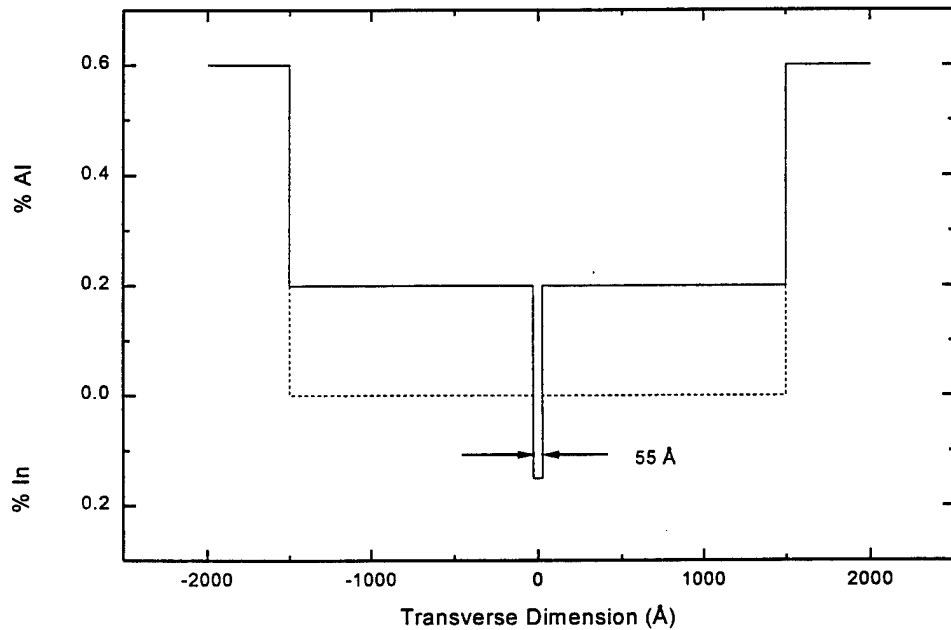


**Figure 2.** Material compositions and layer thicknesses of deep and shallow quantum wells. The deep well is given by the solid line and the shallow well by the dashed line.

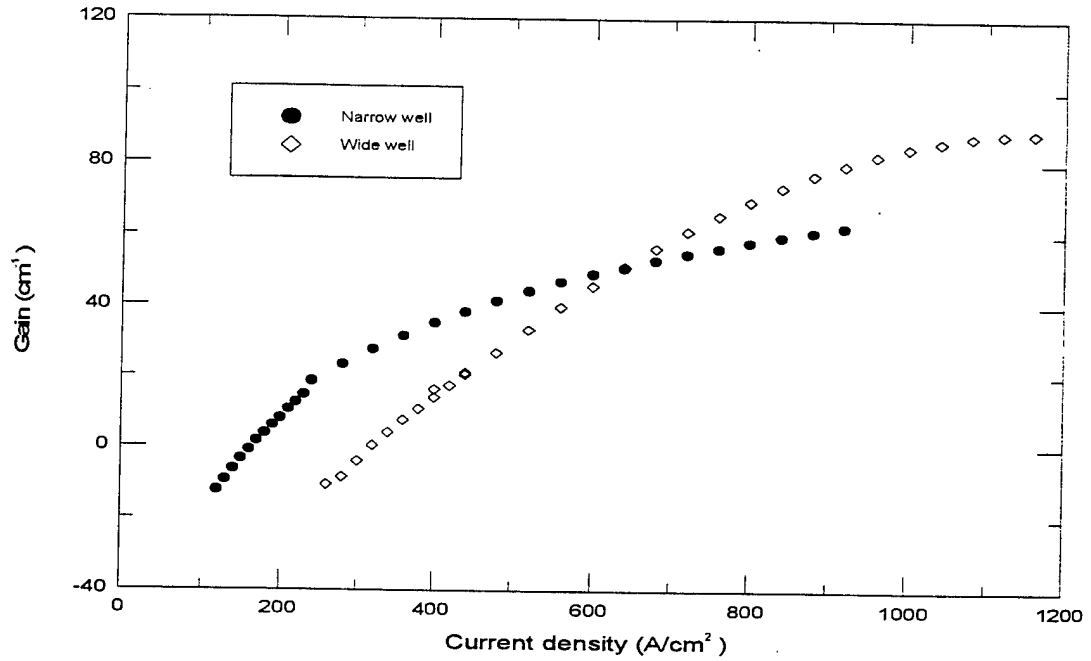


Figure 3. Narrow and wide well gain versus current density.

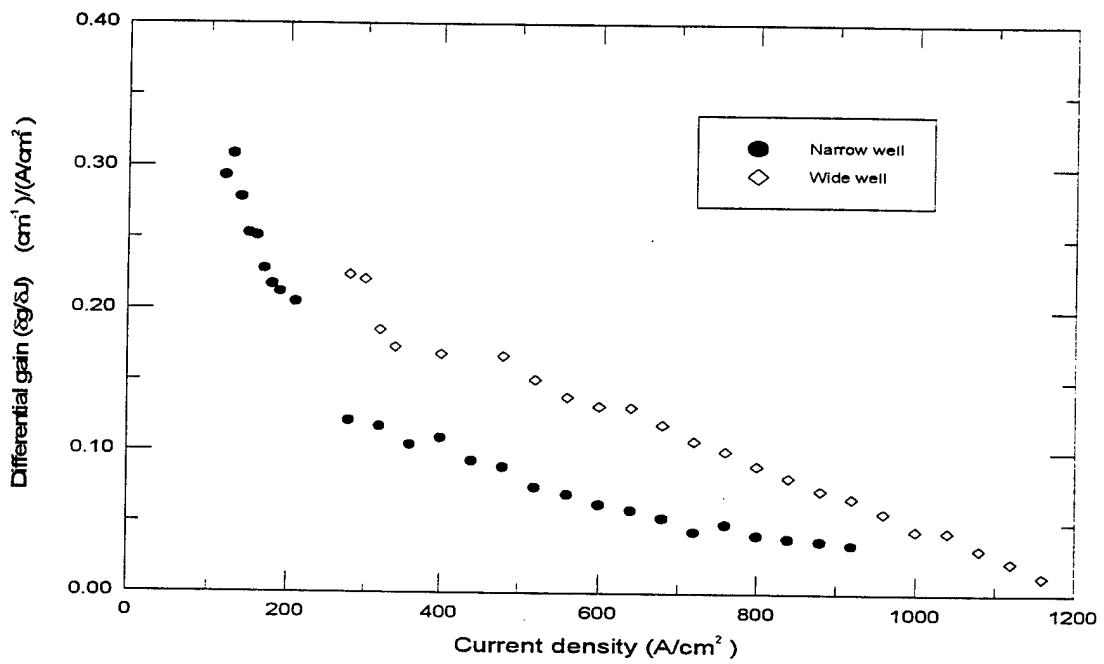


Figure 4. Narrow and wide well differential gain as a function of current density.

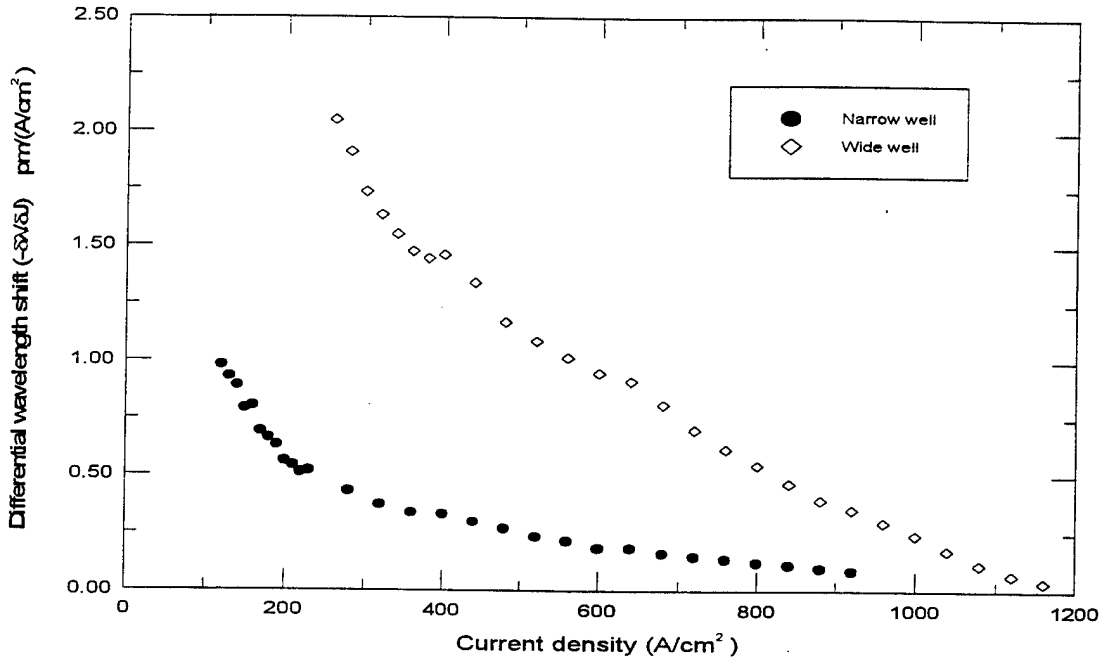


Figure 5. Differential wavelength shift, resulting from refractive index change, versus current density for narrow and wide wells. The wavelength shift is proportional to the refractive index change with carrier density, as seen in Eq. 2.

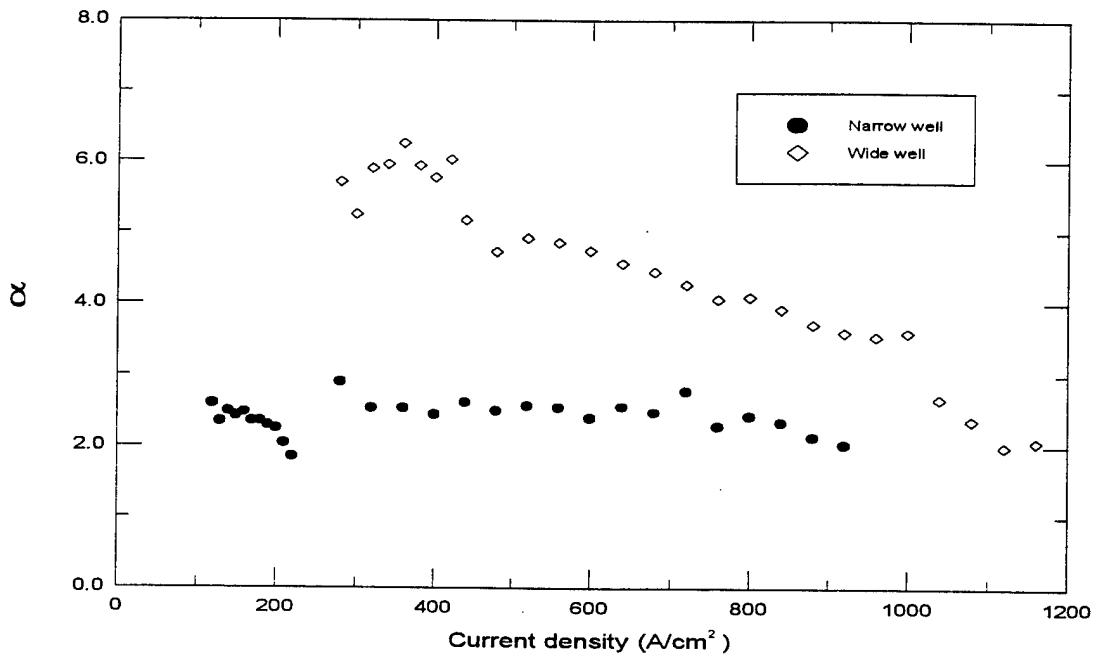


Figure 6. Values of  $\alpha$  versus current density for narrow and wide wells.

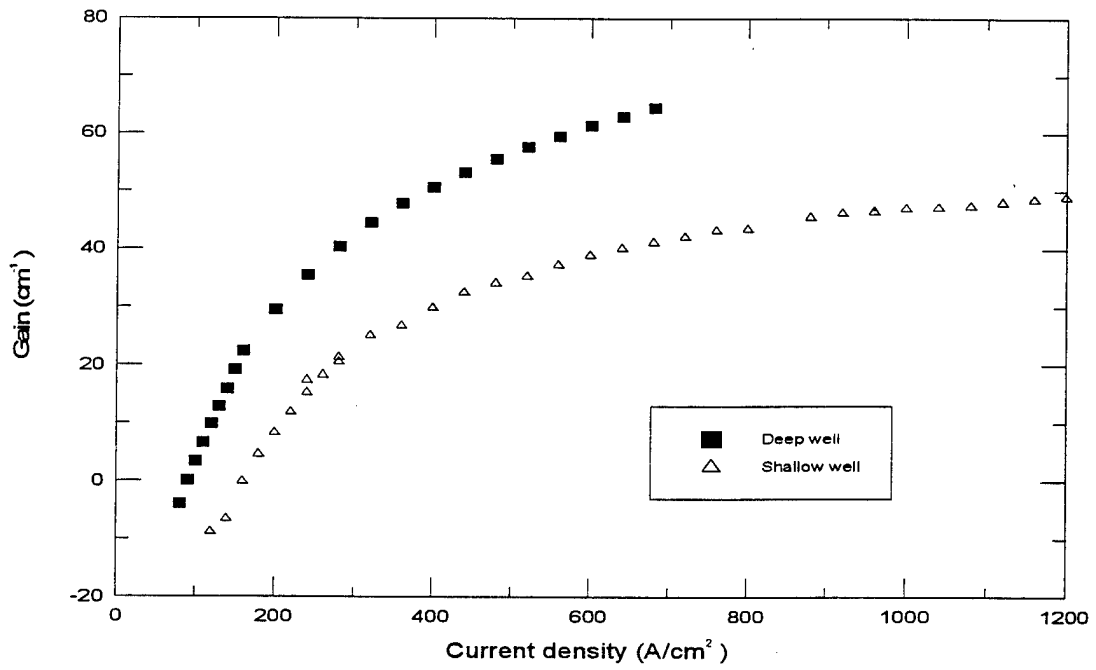


Figure 7. Gain for deep and shallow wells.

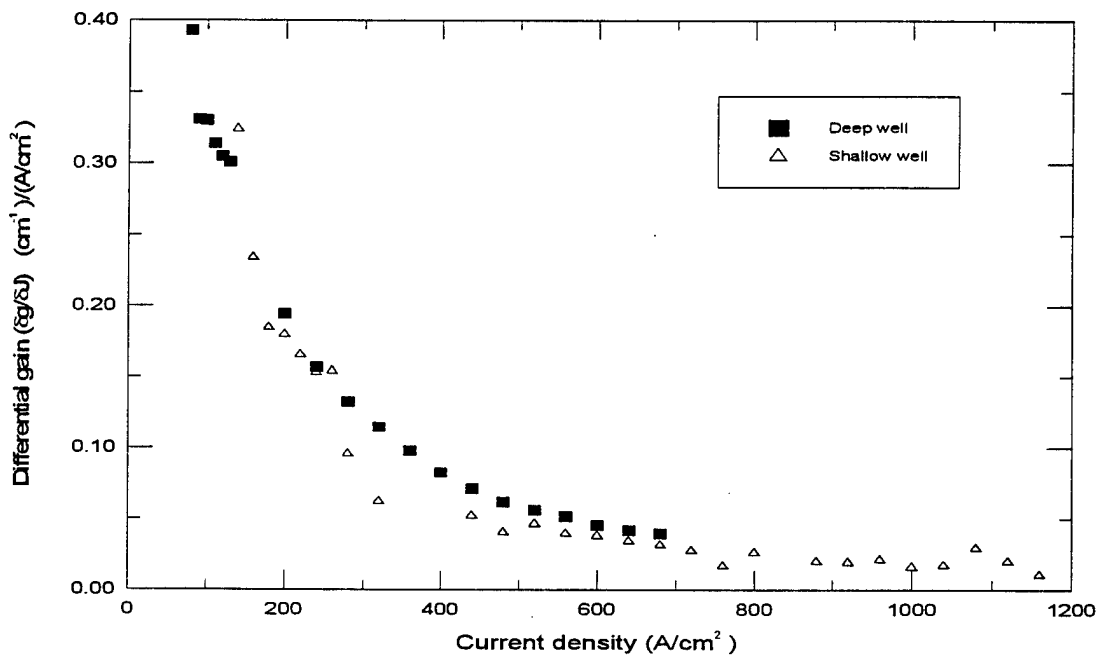


Figure 8. Deep and shallow well differential gain versus current density.

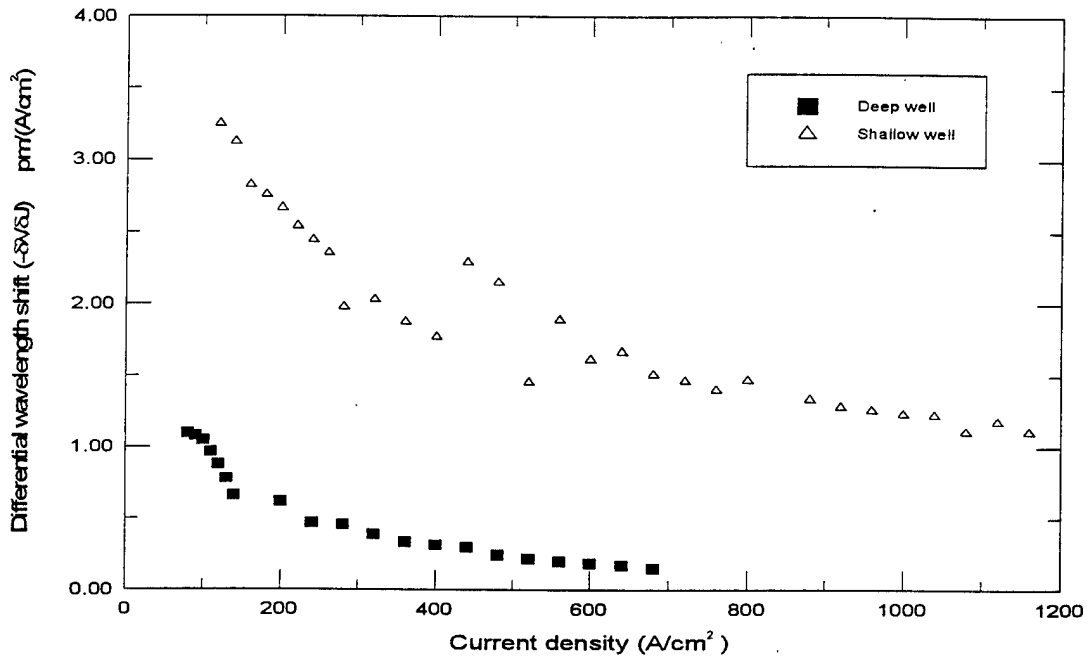


Figure 9. Differential wavelength shift, resulting from refractive index change, for deep and shallow wells.

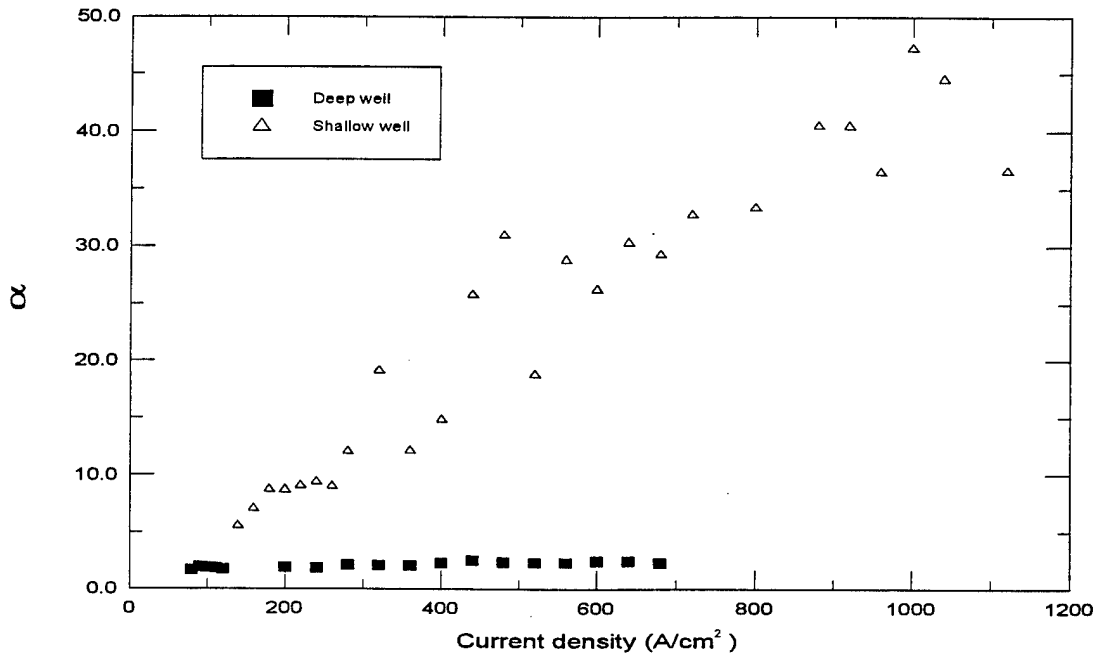


Figure 10. Deep and shallow well  $\alpha$  values versus current density.